

Correlation of InGaP(001) surface structure during growth and bulk ordering

M. Zorn*

Institut für Festkörperphysik, Technische Universität Berlin, Sekr. PN 6-1, Hardenbergstraße 36, D-10623 Berlin, Germany

P. Kurpas

Ferdinand-Braun-Institut für Höchstfrequenztechnik, Albert-Einstein-Straße 11, D-12489 Berlin, Germany

A. I. Shkrebtii

Department of Physics, University of Toronto, Toronto, Canada M5S 1A7

B. Junno

Department of Solid State Physics, Lund University, Box 118, S-221 00 Lund, Sweden

A. Bhattacharya

Ferdinand-Braun-Institut für Höchstfrequenztechnik, Albert-Einstein-Straße 11, D-12489 Berlin, Germany

K. Knorr

Institut für Festkörperphysik, Technische Universität Berlin, Sekr. PN 6-1, Hardenbergstraße 36, D-10623 Berlin, Germany

M. Weyers

Ferdinand-Braun-Institut für Höchstfrequenztechnik, Albert-Einstein-Straße 11, D-12489 Berlin, Germany

L. Samuelson

Department of Solid State Physics, Lund University, Box 118, S-221 00 Lund, Sweden

J. T. Zettler and W. Richter

Institut für Festkörperphysik, Technische Universität Berlin, Sekr. PN 6-1, Hardenbergstraße 36, D-10623 Berlin, Germany

(Received 1 April 1999)

CuPt_B-type ordering of InGaP grown lattice matched to GaAs was investigated by *in situ* reflectance anisotropy spectroscopy and reflection high-energy electron diffraction. The experiments have been performed during InGaP growth both via metal-organic vapor phase epitaxy and chemical beam epitaxy. Additionally, total energy calculations (TE) have been performed for differently ordered InGaP slabs. From both experiment and TE calculations we conclude that bulk ordering only occurs when InGaP growth is performed under phosphorus-rich (2×1)-like surface conditions. Bulk ordering completely disappears under growth conditions which cause a less-phosphorus-rich (2×4)-like surface dimer configuration. P dimers in the (2×1) symmetry at the growth surface trigger the bulk ordering driven by an energy gain of 0.26 eV per surface atom according to our TE calculations. [S0163-1829(99)05635-0]

I. INTRODUCTION

InGaP is an important semiconductor for the fabrication of optoelectronic and electronic semiconductor devices such as heterojunction bipolar transistors (HBTs) (Ref. 1) and diode lasers.² Influenced by the growth conditions, InGaP shows CuPt_B-type ordering on the group-III sublattice. This ordering effect³⁻⁶ results in a reduction of the band gap E_0 (Ref. 7) and a reduced bulk symmetry. It is commonly quantified by an ordering parameter η having values between 0 (for completely disordered material) and 1 (for completely ordered material) thus describing a superlattice consisting of alternating gallium- and indium-rich $\langle 111 \rangle_B$ planes (In_{0.5(1-\eta)}Ga_{0.5(1+\eta)}P/In_{0.5(1+\eta)}Ga_{0.5(1-\eta)}P). Detailed thermodynamical studies by Zhang *et al.*⁸ and Froyen *et al.*⁹ demonstrated that the disordered In_{0.48}Ga_{0.52}P alloy represents the equilibrium state. The InGaP bulk ordered phase is

a metastable configuration corresponding to a total-energy (TE) local minimum. Therefore, CuPt_B-type ordering was related to the surface structure during growth and it has been proposed that phosphorus (P) dimers along the $[\bar{1}10]$ direction promote the ordering process.^{8,10,11} This assumption is based on surface photoabsorption (SPA) investigations¹¹ and theoretical calculations within the valence force-field approach.^{8,10} Philips *et al.*¹⁰ proposed a model based on the assumption that the phosphorus dimers of a (2×X) surface reconstruction produce alternating dilated and compressed lattice rows in the subsurface layers. Since the different atoms which form the ordering sublattice [in this case the group-III atoms gallium (small) and indium (big)] differ in their tetrahedral radii, the occupation of certain sites is biased beneath the strained (2×1) dimer structure.⁸

Both, *n*-type¹² and *p*-type¹³ doping have a strong influence on the ordering behavior of the InGaP layer. Bulk or-

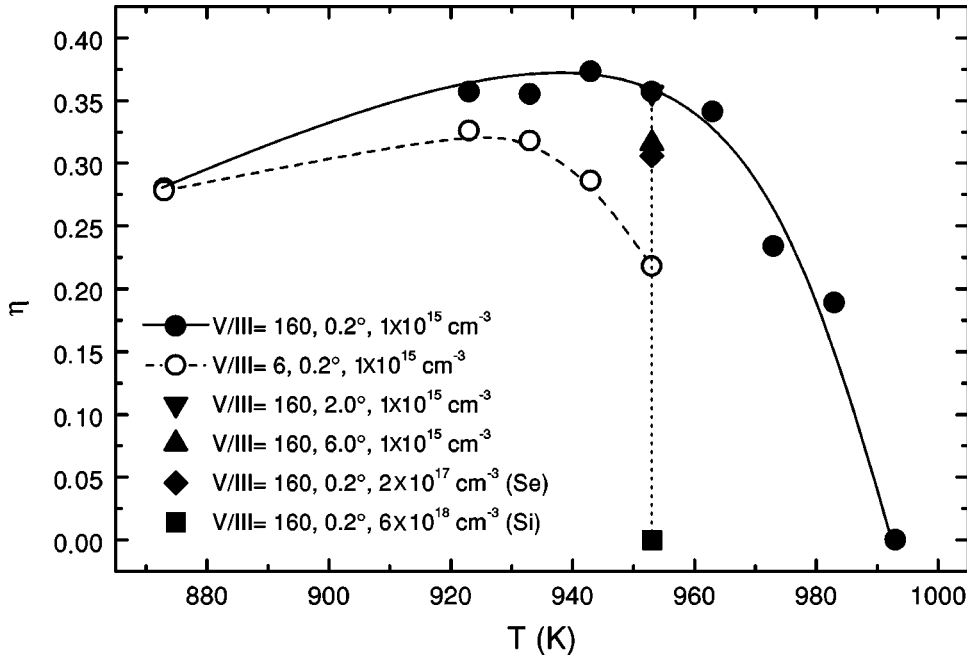


FIG. 1. Dependence of the ordering parameter η on growth temperature for two different V/III ratios. Additionally data for two different off-orientations and two doping concentrations are shown.

dering disappears when the doping level reaches approximately $5 \times 10^{17} \text{ cm}^{-3}$ for *n*-type doped material or $1 \times 10^{18} \text{ cm}^{-3}$ for *p*-type doping. Recently, Lee *et al.*¹⁴ suggested an alternative ordering mechanism while studying the dependence of the ordering parameter η on the InGaP doping level. Based on the observation that step bunching and ordering disappear at the same doping level, the growth of ordered material was correlated to kinetic effects at the step edges.¹⁴

In order to clarify the correlation between bulk ordering and surface structure, we performed systematic reflectance anisotropy spectroscopy (RAS/RDS) (Refs. 15 and 16) studies under metal-organic vapor phase epitaxy (MOVPE) and chemical beam epitaxy (CBE) conditions. RAS studies of the CuPt_B-type ordering in general are complicated due to the difficulty of separating the surface and the bulk contributions to the optical response. Therefore, former RAS investigations^{17–20} could not establish a clear correlation between the surface structure and the bulk ordering. In order to circumvent these problems due to the superposition of bulk and surface anisotropy contributions in our approach, we first separated the bulk dielectric anisotropy that is caused by a certain bulk ordering parameter η . With this knowledge, the surface contribution to the RAS spectra was extracted and its dependence on growth parameters such as temperature, V/III ratio, sample off-orientation, and doping was studied. A clear and unambiguous correlation between the occurrence of the ordering and the presence of a (2×1) surface reconstruction during growth was established by simultaneously performed reflection high-energy electron diffraction (RHEED) and RAS measurements in CBE.

In addition to the experimental studies, we carried out calculations using the density-functional theory within the local-density approximation (DFT-LDA) (Ref. 21) for elucidating in detail the interplay of the during-growth surface dimer configuration and bulk ordering.

II. EXPERIMENT

InGaP layers were grown in two different growth systems: (i) an Aixtron 200 MOVPE system and (ii) a chemical

beam epitaxy (CBE) system equipped with a RHEED (Ref. 22) facility. In both systems growth was monitored by a RAS spectrometer²³ attached to the growth chamber via a low-strain optical window.²⁴ Phosphine (PH_3), trimethylgallium (TMGa), trimethylindium (TMIn), disilane (H_2Si_2), and hydrogen selenide (H_2Se) were used as precursors for the MOVPE experiments; bisphosphinoethane (BPE), triethylgallium (TEGa), and trimethylindium (TMIn) were the source materials for CBE growth. InGaP layers were grown on semi-insulating GaAs(001) substrates slightly off-oriented (0.2°) towards $(111)B$. Samples with an off-orientation of (2°) towards $(111)B$ and (6°) towards $(111)A$ were additionally used for comparison. The ordering parameter was estimated by room-temperature photoluminescence (PL) on $0.65\text{-}\mu\text{m}$ and $1.3\text{-}\mu\text{m}$ -thick InGaP layers from the difference $\Delta E_0 = E_0^{\text{disordered}} - E_0^{\text{ordered}}$ of the measured band gap (E_0^{ordered}). The respective value for disordered InGaP ($E_0^{\text{disordered}}$) was calculated using an empirical equation according to Stringfellow:²⁵

$$E_0^{\text{disordered}} = 2.78 - 2.13x + 0.7x^2, \quad (1)$$

with x being the indium content determined via x-ray diffraction. From the band-gap reduction ΔE_0 , the ordering parameter η was estimated according to Ernst *et al.*:²⁶

$$\eta = \sqrt{\frac{\Delta E_0}{471 \text{ meV}}}. \quad (2)$$

The reflectance anisotropy was measured as the difference in reflectance between the two surface symmetry axes along $[\bar{1}10]$ and $[110]$:

$$\frac{\Delta r}{r} = 2 \frac{r_{[\bar{1}10]} - r_{[110]}}{r_{[\bar{1}10]} + r_{[110]}}. \quad (3)$$

III. THEORETICAL DETAILS

Both the InGaP(001) surface geometry and the corresponding relaxation of bulk atoms with respect to the ideal zinc-blende configuration have been determined by TE minimization using DFT-LDA. In order to model the growth of the Ga, In, and P containing layers, we have considered a (001) periodic slab of ten atomic layers plus a vacuum region equivalent in thickness to eight atomic layers. To preserve the GaAs substrate bulklike environment, the last two layers of the slab have been fixed in a bulklike ideal position, while the back side of the slab has been saturated by fictitious, fractionally charged H atoms. Single-particle orbitals are expanded into plane waves up to an energy cutoff of 10 Ry. Four special k points have been used in the irreducible part of the two-dimensional surface Brillouin zone. Atomic coordinates have been relaxed using the Car-Parrinello molecular-dynamics scheme.²⁷ We have used theoretical GaAs bulk constants and a 50/50 In/Ga ratio, close to the 0.48/0.52 experimental one. The atomic structure of the InGaP layers deep beneath the surface has been compared to the atomic structure of bulk InGaP, which has been minimized in a separate run, using a supercell with 32 atoms.

It will be shown in the experimental part that only the phosphorus-rich (2×1) phase produces the high degree of InGaP bulk ordering. Hence, we focused on the modeling of the (2×1)-like P-dimer structure. The $p(2 \times 2)$ supercell chosen in the calculations is compatible with the phosphorus-rich (2×1) reconstruction.

IV. RESULTS AND DISCUSSION

A. Dependence of the ordering on growth parameters

The degree of bulk ordering in InGaP is known to depend on basically all the main growth parameters.^{12–14,28,29} Therefore, we varied the bulk ordering by systematically changing the growth parameters as shown in Fig. 1.

(i) *Temperature variation.* Starting from a medium value, the ordering increases with increasing temperature until reaching a maximum η around 935 K. Further increase in temperature reduces the ordering until it vanishes at very high temperatures.

(ii) *V/III-ratio variation.* The ordering decreases with decreasing V/III ratio.

(iii) *Off-orientation.* The ordering parameter is basically the same for surface off-orientations of 0.2° and 2° towards (111) B but it decreases when the off-orientation is changed to 6° towards (111) A .

(iv) *Doping.* The ordering is the highest for undoped InGaP. When the layers are n -type doped with Se or Si, η decreases ($n = 2 \times 10^{17} \text{ cm}^{-3}$) and finally vanishes at very high doping levels ($n = 6 \times 10^{18} \text{ cm}^{-3}$).

All these dependences on different growth conditions can be traced back to a single reason: the surface dimer configuration during growth.

B. Ordering-induced bulk anisotropy

In order to distinguish between surface (reconstruction) and bulk (ordering) contributions to the RAS spectra, first the bulk anisotropy was measured separately. It can be assumed that the anisotropy contribution from the oxidized

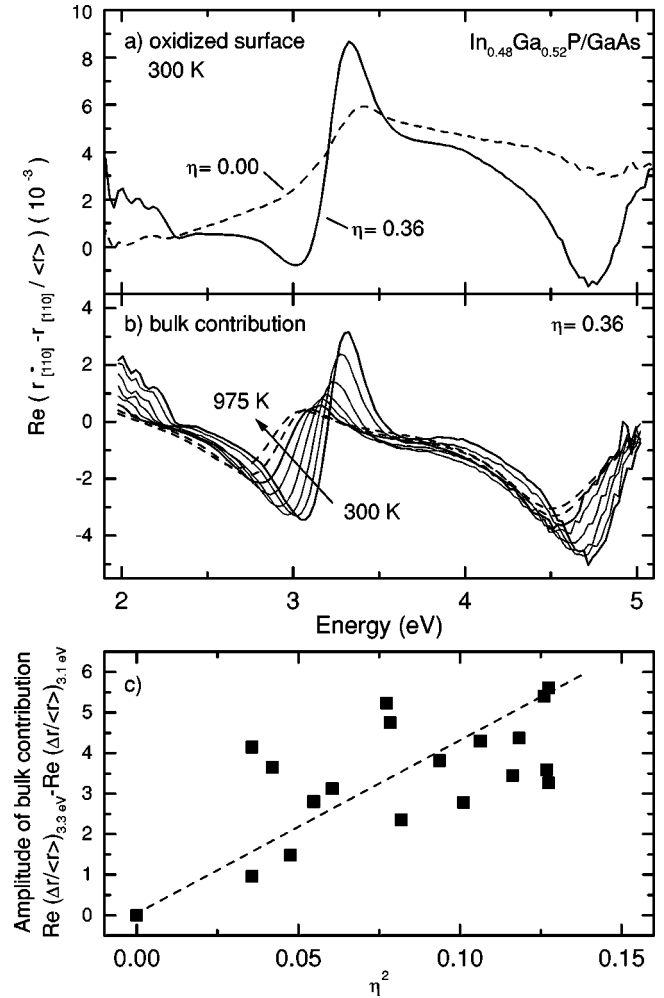


FIG. 2. (a) RAS spectra of oxidized In_{0.48}Ga_{0.52}P layers for an ordered ($\eta = 0.36$) and a disordered sample ($\eta = 0$) at 300 K. (b) Temperature-dependent bulk contribution to the reflectance anisotropy for $\eta = 0.36$ between 300 K and 975 K. The spectra at 875 K and 975 K (dashed lines) are extrapolated from the measured data. (c) Dependence of the amplitude of the bulk anisotropy in the RAS spectra from the ordering parameter η at 300 K.

InGaP surface is only small and independent from the bulk ordering. Therefore, differently ordered InGaP layers were oxidized and heated under N₂ flow since the oxide layers are stable up to 775 K under these conditions. The bulk contribution of the ordered InGaP layers to their RAS spectra was separated then by subtracting the RAS spectrum of a disordered reference sample (caused by the oxide/InGaP interface only).

In Fig. 2(a), the RAS spectra of oxidized ordered ($\eta = 0.36$) and disordered layers at room temperature are shown. The bulk anisotropy obtained by the above-described approach is shown in Fig. 2(b) for temperatures between room temperature and 975 K. These spectra display a characteristic line shape with a maximum around 3.3 eV and two minima around 3 eV and 4.6 eV at room temperature. The spectra at 875 K and 975 K are extrapolated from the measured data using the temperature dependence of the InGaP bulk dielectric function since above 800 K the oxide starts to desorb. It has been shown that the corresponding bulk dielectric anisotropy resembles the first derivative of the averaged

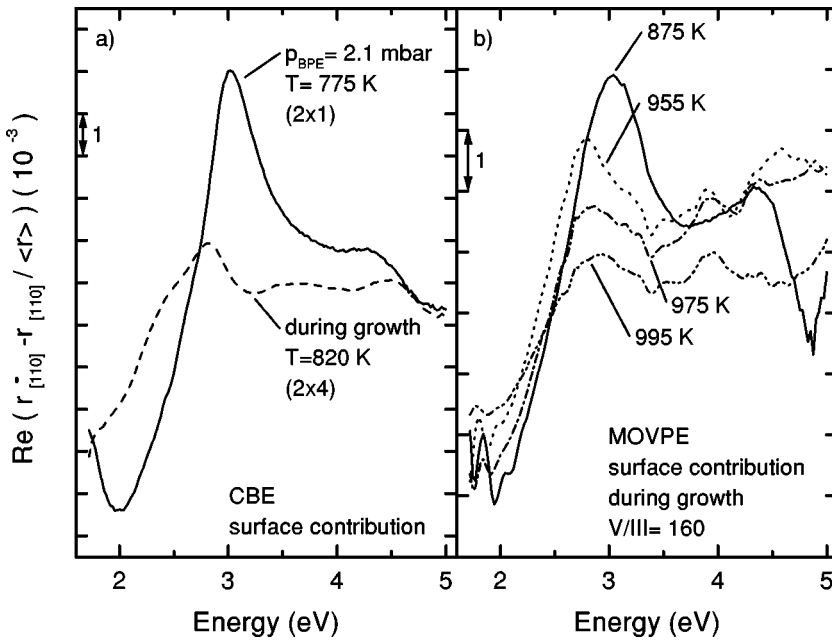


FIG. 3. Comparison of $\text{In}_{0.48}\text{Ga}_{0.52}\text{P}$ RAS spectra taken under (a) CBE and (b) MOVPE conditions. These spectra reflect the surface contribution only since the bulk contribution is subtracted (see text for details). In both systems the same two characteristic line shapes are measured under P-rich and group-III-rich conditions, respectively. They correspond to a (2×1) and a (2×4) reconstructed $\text{InGaP}(001)$ surface according to their RHEED patterns taken in CBE.

InGaP bulk dielectric function¹⁹ and is therefore caused by an ordering-induced splitting of all the main optical gap energies (E_0 , E_1 , E'_0 , and E_2). In Fig. 2(c), the amplitude of the peak around 3.2 eV in the room-temperature RAS spectra is plotted over the square of the ordering parameter η for the samples grown under different conditions. The amplitude was determined by taking the difference between the RAS value at 3.3 eV (maximum) and 3.1 eV (minimum). This RAS amplitude is proportional to the square of the ordering parameter η . This is not surprising because η is correlated to the square root of the ordering-induced splitting (causing a downshift of the PL energy) of the fundamental band gap E_0 [Eq. 2] and the 3.2-eV RAS signature is correlated to the respective ordering-induced splitting of the E_1 optical gap.¹⁹

C. Correlation of RAS spectra to surface reconstructions

In order to prove the assumption that the surface reconstruction during growth influences the ordering parameter,²⁸ RAS spectra were taken while systematically varying the growth temperature, the V/III ratio, the sample off-orientation, and the doping concentration.

In the CBE system, simultaneous RAS and RHEED measurements were performed in order to correlate the RAS spectra to the respective surface reconstructions. Two surface reconstructions have been found on $\text{InGaP}(001)$ similar to its binary boundary systems $\text{InP}(001)$ (Refs. 30 and 31) and $\text{GaP}(001)$:³² a (2×1) reconstruction under high phosphorus pressure and a (2×4) symmetry during growth, i.e., under group-III-rich conditions. In contrast to the binary phosphorus compounds InP and GaP where the (2×4) surface reconstruction can also be found under static conditions at low phosphorus supply, for InGaP in our experiments this reconstruction showed up during growth only. $\text{InGaP}(001)$ surfaces of (2×1) symmetry have also been reported in gas-source molecular-beam epitaxy (GSMBE) (Ref. 33), and in solid-source molecular-beam epitaxy (SSMBE).³⁴ A (2×4) reconstruction was found during growth on InGaP under low phosphine flow rates in metal-organic molecular-beam epitaxy (MOMBE).³⁵

The surface contributions to the RAS spectra of the (2×1) and the (2×4) surface reconstruction are shown in Fig. 3(a). They differ characteristically in the energy range around 3 eV. The spectrum of the (2×1) reconstructed surface consists of a sharp peak at 3 eV while this peak nearly vanishes in the case of (2×4) surface reconstruction.

Under MOVPE conditions, very similar RAS spectra can be observed, e.g., by varying the growth temperature. This indicates that under gas-phase conditions also a (2×1) -like and a (2×4) -like surface dimer configuration are present under phosphorus-rich and under group-III-rich conditions, respectively. Figure 3(b) shows RAS spectra taken during growth at a V/III ratio of 160 in the temperature range between 875 K and 995 K showing significant changes when the temperature is increased.

These changes from the (2×1) -like to (2×4) -like RAS signatures are caused by the enhanced desorption of phosphorus at high temperatures leading to group-III-rich conditions and a decrease in the RAS signal at 2.9 eV.

D. Correlation of during-growth surface reconstruction and resulting degree of ordering

With the surface status during growth known from its characteristic contribution to the RAS spectra, it is possible to establish a correlation between the during-growth surface dimer configuration and the resulting degree of ordering. This is done in Fig. 4, where the data of the samples investigated in Fig. 1 are plotted over the RAS amplitude at 2.9 eV that serves here as a measure for the domain ratio of (2×1) -like and (2×4) -like surface dimer configurations during growth. The result is clear and unambiguous: The ordering is influenced by all growth parameters via the surface reconstruction.

(i) *Sample temperature.* With increasing sample temperature, the ordering parameter η decreases for temperatures between 925 K and 995 K.

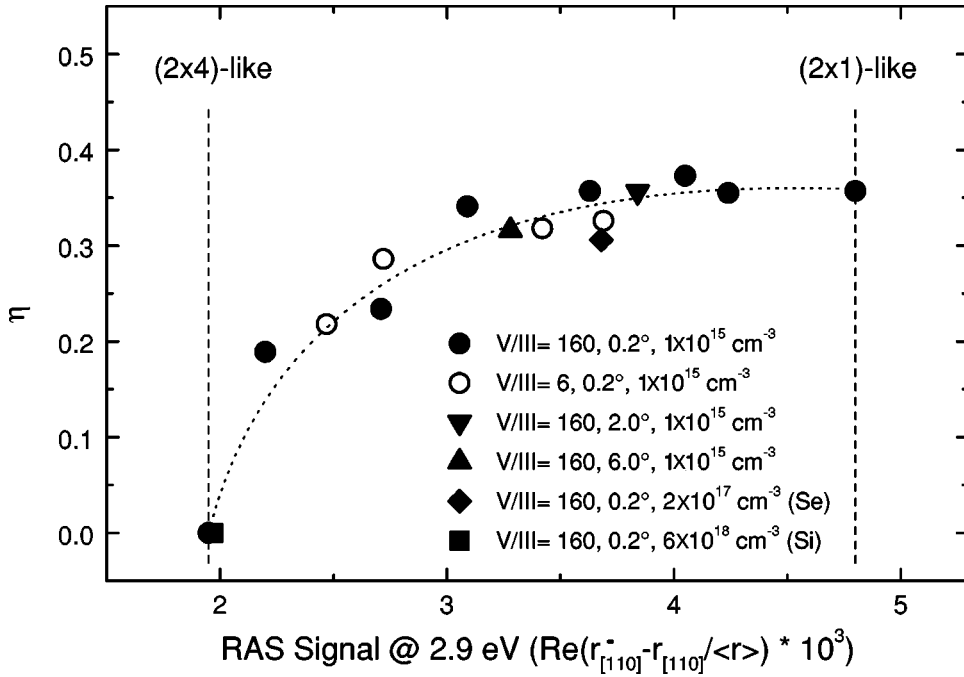


FIG. 4. Correlation of ordering parameter η to the RAS amplitude at 2.9 eV (surface contribution only) that scales with the $(2 \times 1)/(2 \times 4)$ surface domain ratio. The data from Fig. 1 are used here (V/III ratio, sample off-orientations, doping concentrations, and temperature varied between 925 K and 995 K).

(ii) *V/III ratio.* At lower V/III ratios the surface chemical potential of phosphorus is reduced. The RAS value at 2.9 eV mirrors the respective crossover to (2×4) -like group-III-rich surface conditions.

(iii) *Sample off-orientation.* When the off-orientation is increased from 0.2° to 2° [both towards $(111)B$], no significant change either in the ordering or in the RAS signal can be observed. However, changing the off-orientation to 6° [towards $(111)A$] causes the surface to become group III rich due to the increasing number of steps supporting the desorption of group-V atoms [as reported for GaAs (Ref. 36)] and consequently both the ordering and the RAS signal decrease.

(iv) *n-doping.* The ordering decreases with increasing doping concentration ($n = 2 \times 10^{17} \text{ cm}^{-3}$) and disappears at high doping levels ($n = 6 \times 10^{18} \text{ cm}^{-3}$) as reported.^{12,14}

In conclusion, InGaP CuPt_B-bulk ordering is caused by growth conditions where the growth surface is covered by (2×1) -like surface dimers. Ordering disappears when the growth surface is covered by (2×4) -like surface dimers.

Depending on the growth conditions, the (2×1) is present under phosphorus-rich conditions indicating that this surface consists of phosphorus dimers oriented along the $[\bar{1}10]$ direction. These dimers obviously trigger the bulk ordering by creating strain in the layers just below the surface as has been suggested by Philips *et al.*¹⁰ The occupation of certain lattice sites by gallium and indium is therefore biased due to their different size (see Fig. 5). From detailed studies of the InP(001)- (2×4) and GaP(001)- (2×4) reconstruction^{32,37,38} it is known that this surface should not consist of phosphorus dimers. This explains the disappearance of ordering under group-III-rich growth conditions.

In order to prove this assumption we modeled the InGaP ordering for the P-rich surface phase growth, using the (2×1) P-dimer structure. P dimers were oriented along the $[\bar{1}10]$ direction. We calculated the TE difference ΔE for the (2×1) dimer phase on the InGaP(001) surface between two types of layers: (i) using a structure that follows the subsur-

face selectivity rule (Fig. 5: small Ga atoms under the strained dimer rows and large In atoms between the dimer rows), and (ii) using a configuration antisymmetric to the subsurface selection rule (large In atoms under the strained dimer rows and small Ga atoms between the dimer rows). We found, starting from the zero ΔE for the two InGaP layers, that a TE difference of 0.24 eV per surface atom for these two "opposite" structures is reached even for four InGaP layers. ΔE saturates at 0.26 eV per surface atom for six, eight, or ten InGaP layers.

Finally, as can be seen in Fig. 5, we have found that P dimers are asymmetric for the (2×1) phase because they are

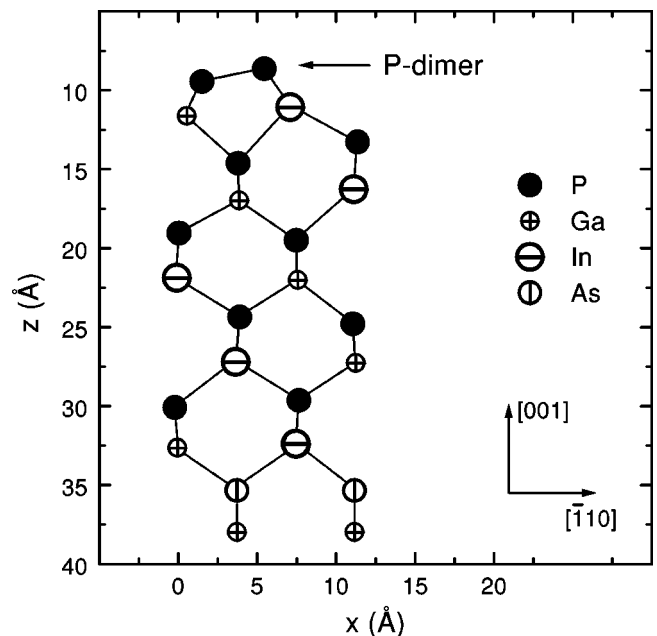


FIG. 5. Calculated atomic positions of the subsurface InGaP crystal using the DFT-LDA-based TE minimization. The resulting buckling of the P dimer can clearly be seen.

connected to the chemically nonequivalent atoms with different covalent radii. The P-dimer buckling is 0.42 \AA , while dimer length is 2.16 \AA , close to the sum of the phosphorus covalent radii. From the theoretical analysis a clear conclusion can be drawn: the (2×1) P-dimer phase favors bulk ordering in agreement with the above physical arguments. This is in direct contrast to results published in Ref. 11, where phosphorus dimers were supposed to be likely for the (2×4) -like surfaces.

However, at lower temperatures, where the surface is always phosphorus-rich and (2×1) -like due to the reduced phosphorus desorption, the ordering is slightly reduced. It can be assumed that the P-dimer driven ordering, i.e., the diffusion of indium and gallium atoms to their energetically preferred lattice sites in the third subsurface atomic layer, is kinetically hindered under this conditions and therefore the

degree of ordering is reduced when growth is performed at low temperatures.

V. CONCLUSIONS

A direct and unambiguous correlation between the resulting degree of ordering and the during growth surface dimer configuration was established. Ordering occurs under (2×1) -like surfaces and vanishes under (2×4) -like surface conditions. Total-energy calculations confirm that the P dimers in the (2×1) symmetry trigger bulk ordering driven by an energy gain of 0.26 eV per surface atom.

ACKNOWLEDGMENTS

The authors gratefully acknowledge support by the BMBF (01 BT 310/835), the DAAD, and the SFB 296.

-
- *Electronic address: zorn@physik.tu-berlin.de; Fax: 49-30-31421769.
- ¹S.S. Lu and C.C. Huang, IEEE Electron Device Lett. **13**, 214 (1992).
 - ²L.J. Mawst, A. Bhattacharya, J. Lopez, D. Botez, D.Z. Garbuzow, L. DiMarco, J.C. Conolly, M. Jansen, F. Fang, and R. Nabiev, Appl. Phys. Lett. **69**, 1532 (1996).
 - ³A. Gomyo, K. Kobayashi, S. Kawata, I. Hino, T. Suzuki, and T. Yuasa, J. Cryst. Growth **77**, 367 (1986).
 - ⁴A. Zunger and S. Mahajan, in *Handbook on Semiconductors* (Elsevier Science B.V., Amsterdam, 1994), Vol. 3, Chap. 19.
 - ⁵C. Geng, Ph.D. thesis, University of Stuttgart, 1997.
 - ⁶I. Pietzonka, T. Sass, R. Franzheld, G. Wagner, and V. Gottschalch, J. Cryst. Growth **195**, 21 (1998).
 - ⁷A. Gomyo, T. Suzuki, and S. Iijima, Phys. Rev. Lett. **60**, 2645 (1988).
 - ⁸S.B. Zhang, S. Froyen, and A. Zunger, Appl. Phys. Lett. **67**, 3141 (1995).
 - ⁹S. Froyen and A. Zunger, Phys. Rev. B **53**, 4570 (1996).
 - ¹⁰B.A. Philips, A.G. Norman, T.Y. Seong, S. Mahajan, G.R. Booker, M. Skowronski, J.P. Harbison, and V.G. Keramidas, J. Cryst. Growth **140**, 249 (1994).
 - ¹¹H. Murata, I.H. Ho, L.C. Su, Y. Hosokawa, and G.B. Stringfellow, J. Appl. Phys. **79**, 6895 (1996).
 - ¹²A. Gomyo, H. Hotta, I. Hino, S. Kawata, K. Kobayashi, and T. Suzuki, Jpn. J. Appl. Phys., Part 2 **28**, L1330 (1989).
 - ¹³T. Suzuki, A. Gomyo, I. Hino, K. Kobayashi, S. Kawata, and S. Iijima, Jpn. J. Appl. Phys., Part 2 **27**, L1549 (1988).
 - ¹⁴S.H. Lee, T.C. Hsu, and G.B. Stringfellow, J. Appl. Phys. **84**, 2618 (1998).
 - ¹⁵D.E. Aspnes, Mater. Sci. Eng., B **30**, 109 (1995).
 - ¹⁶M. Zorn, J. Jönsson, W. Richter, J.-T. Zettler, and K. Ploska, Phys. Status Solidi A **152**, 23 (1995).
 - ¹⁷J.S. Luo, J.M. Olson, S.R. Kurtz, D.J. Arent, K.A. Bertness, M.E. Raikh, and E.V. Tsiper, Phys. Rev. B **51**, 7603 (1995).
 - ¹⁸B.A. Philips, I. Kamiya, K. Hingerl, L.T. Florez, D.E. Aspnes, S. Mahajan, and J.P. Harbison, Phys. Rev. Lett. **74**, 3640 (1995).
 - ¹⁹J.-T. Zettler, Prog. Cryst. Growth Charact. Mater. **35**, 27 (1997).
 - ²⁰J.S. Luo, J.F. Geisz, J.M. Olson, and M.-C. Wu, J. Cryst. Growth **174**, 558 (1997).
 - ²¹W. Kohn and L.J. Sham, Phys. Rev. **140**, A1133 (1965).
 - ²²B.A. Joyce, Rep. Prog. Phys. **48**, 1637 (1985).
 - ²³D.E. Aspnes, R. Bhat, E. Colas, L.T. Florez, J.P. Harbison, M.K. Kelly, V.G. Keramidas, M.A. Koza, and A.A. Studna, Proc. SPIE **1037**, 2 (1988).
 - ²⁴A.A. Studna, D.E. Aspnes, L.T. Florez, B.J. Wilkens, J.P. Harbison, and R.E. Ryan, J. Vac. Sci. Technol. A **7**, 3291 (1989).
 - ²⁵G.B. Stringfellow, J. Appl. Phys. **43**, 3455 (1972).
 - ²⁶P. Ernst, C. Geng, F. Scholz, H. Schweizer, Y. Zhang, and A. Mascarenhas, Appl. Phys. Lett. **67**, 2347 (1995).
 - ²⁷M. Bockstedte, A. Kley, J. Neugebauer, and M. Scheffler, Comput. Phys. Commun. **107**, 187 (1997).
 - ²⁸A. Gomyo, T. Suzuki, K. Kobayashi, S. Kawata, I. Hino, and T. Yuasa, Appl. Phys. Lett. **50**, 673 (1987).
 - ²⁹K. Sinha, A. Mascarenhas, R.G. Alonso, G.S. Horner, K.A. Bertness, S.R. Kurtz, and J.M. Olson, Solid State Commun. **89**, 843 (1994).
 - ³⁰M. Zorn, T. Trepk, J.-T. Zettler, B. Junno, C. Meyne, K. Knorr, T. Wethkamp, M. Klein, M. Miller, W. Richter, and L. Samuelson, Appl. Phys. A: Mater. Sci. Process. **65**, 333 (1997).
 - ³¹K.B. Ozanyan, P.J. Parbrook, M. Hopkinson, C.R. Whitehouse, Z. Sobiesierski, and D.I. Westwood, J. Appl. Phys. **82**, 474 (1997).
 - ³²M. Zorn, B. Junno, T. Trepk, S. Bose, L. Samuelson, J.-T. Zettler, and W. Richter, Phys. Rev. B (to be published).
 - ³³J.H. Quigley, M.J. Hafich, H.Y. Lee, R.E. Stave, and G.Y. Robinson, J. Vac. Sci. Technol. B **7**, 358 (1989).
 - ³⁴T. Shitara and K. Eberl, Appl. Phys. Lett. **65**, 356 (1994).
 - ³⁵J.Ch. Garcia, Ph. Maurel, Ph. Bove, and J.P. Hirtz, J. Appl. Phys. **69**, 3297 (1991).
 - ³⁶K. Ploska, M. Pristovsek, W. Richter, J. Jönsson, I. Kamiya, and J.-T. Zettler, Phys. Status Solidi A **152**, 49 (1995).
 - ³⁷W.G. Schmidt, F. Bechstedt, N. Esser, M. Pristovsek, Ch. Schultz, and W. Richter, Phys. Rev. B **57**, 14 596 (1998).
 - ³⁸A.M. Frisch, W.G. Schmidt, J. Bernholc, M. Pristovsek, N. Esser, and W. Richter, Phys. Rev. B **60**, 2488 (1999).